Mecánica Computacional Vol. XXI, pp. 2475–2486
S. R. Idelsohn, V. E. Sonzogni and A. Cardona (Eds.)
Santa Fe–Paraná, Argentina, October 2002

A COMPARISON BETWEEN THE STRESS DISTRIBUTION IN ANGLED AND VERTICAL IMPLANTS

Estevam B. de Las Casas[*], Paulo C. Ferreira[*], Carlos A. Cimini Jr. [*], Elson M. Toledo[†§], Luis Paulo S. Barra[†] and Mauro Cruz[**]

[*]Escola de Engenharia, Universidade Federal de Minas Gerais
Av. do Contorno, 842, Centro, Belo Horizonte, Minas Gerais, Brasil
e-mail: estevam@dees.ufmg.br, web page: http://www.dees.ufmg.br/biomec

[†]Núcleo de Pesquisa em Métodos Computacionais em Engenharia (NUMEC)
Universidade Federal de Juiz de Fora, Cidade Universitária, Juiz de Fora, Minas Gerais, Brasil
e-mail: luisp@numec.ufjf.br, web page: http://www.numec.ufjf.br

[§]Laboratório Nacional de Computação Científica-LNCC
Av. Getúlio Vargas, 333, Quitandinha, Petrópolis, Rio de Janeiro, Brasil
e-mail: emtc@lncc.br, web page: http://www.lncc.br

[**]Centro Clínico de Pesquisa e Desenvolvimento em Estomatologia (CLINEST)
Av. Rio Branco, 2288, sala 1203, Centro, Juiz de Fora, Minas Gerais, Brasil
e-mail: clinest@terra.com.br, web page: http://www.clinestpq.com.br

Key words: Angled dental implants, stress analysis, biomechanics, mandible.

Summary. *This paper describes the stress distribution in implants of different shapes, based on a three dimensional solid computational model. The geometry of the mandible was obtained from a computerized tomography scan and two different designs for the implant were considered, both part of the Bioform® system produced by Maxtron (Juiz de Fora, Brazil). The first implant is vertical, as commonly used in dentistry practice, and the second has an angled form. The geometric model for each implant was treated through the use of Boolean operations in the region of the first lower molar of the model for the mandible. The resulting geometry served as basis for the discrete finite element model, and a 100 N load was considered, acting first in the vertical and then in the horizontal direction. For a correct description of the forces acting during the masticatory process, the external loads were balanced by the muscular forces acting on the mandible and reaction forces in the line joining the temporomandibular articulations. A discussion is presented on the effectiveness of the different implant forms in the transmission of forces to the mandible.*

1 INTRODUCTION

Different types of implants have been proposed in an attempt to provide a sound mechanical basis for aesthetical and functional solutions in case of partial or total loss of teeth. Angled implants are a quite recent solution aiming at a better adjustment of the implant shape to physiological bone characteristics, without decrease in functionality. A typical situation where such solution could be considered is to avoid interference of the alveolar nerve at the molar region of the mandible.

Bioform® implants are among the pioneers in angled implants. In the same line, vertical models are available with heights ranging from 9 to 17 mm, and diameters between 3,3 and 6,2 mm. As for angled implants, two different variations are available. Both have a cylindrical cross section in the post cervical region. The first type, object of this study, is inclined around the larger axis of its cylindrical cross section (frontal angled implants). Their height varies from 13 to 15 mm, with inclination between 25 and 55°. Alternatively, a laterally angled design is also available (lateral angled implant), this time inclined around the smaller axis. Implants of intermediate dimensions were picked for the analysis described in this paper. For the vertical implant, a 4 mm diameter and 13 mm height, while for the frontal angled implant the diameter at the cervical portion was 4 mm, height of 14 mm and angle of 35°.

The variation from the straight form in the angled implant tends to introduce higher stress levels due to bending. The authors opted for studying the situation where the implant, in their two alternative shapes, were used in the region of the first lower molar The resulting stress distributions in the vicinity of the implant for both design alternatives are discussed for vertical and horizontal loads.

2 COMPUTATIONAL MODELS

For the generation of the solid model, the CT scan of a mandible was used. Thirty-eight sections of the tomography were digitalized and used as input for the preprocessor of the commercial code Ansys®. The coordinates of the points in the available sections served as basis for the generation of lines, defining the contour surfaces and resulting solid model which describes the mandible shape, including the internal boundary between trabeculae and cortical bones.

The implant geometric data was provided by the manufacturer. The solid model resulting from the Boolean intersection of implant and mandible represents the assumption of complete osseointegration, restricting any relative displacement between implant and bone. Another characteristic of the model is the inclusion of a 1 mm layer of cortical bone around the implant. This layer normally grows after complete integration of the piece, resulting from the strain distribution during the first phases of curing[1].

Figure 1 shows a cross section of the model depicting the angled and vertical implants. The considered mechanical properties for the materials and tissues are listed in Table 1, for linear isotropic behavior.

Material	Modulus of Elasticity (MPa)	Poisson ratio
Implant and abutment (titanium)[2]	110.000	0,33
Cortical bone[2,3,4]	13.700	0,30
Trabeculae bone[2,3,4]	1.370	0,30

Table 1: Material mechanical properties.

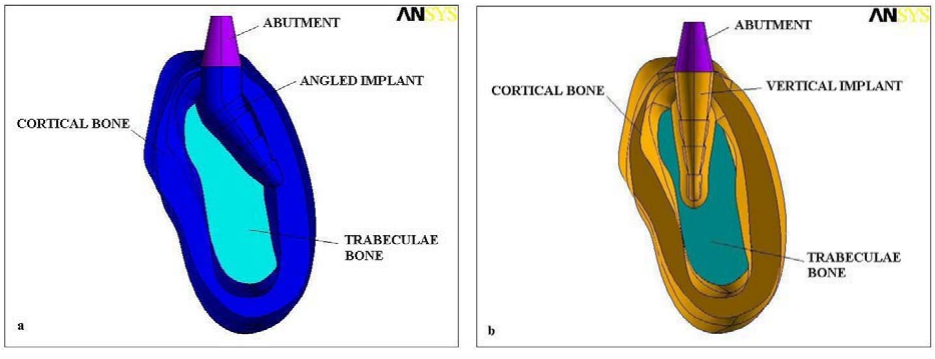

Figure 1: Position of angled (a) and vertical (b) implants.

3 LOADS AND BOUNDARY CONDITIONS

Two different load cases for each of the two configurations were considered:

- Vertical implant subjected to vertical load;
- Vertical implant subjected to horizontal load;
- Horizontal implant subjected to vertical load;
- Horizontal implant subjected to vertical load.

The 100 kN load was applied at the central node in the upper surface of the abutment. In addition to the implant load, the forces of the main muscles active in the mastication process were also considered. The approach was previously used by Inou[5] , and the forces were taken to be proportional in modulus to the cross sectional area of the muscle. The considered muscles were the Masseter (M), Middle (or internal) Pterygoid (MP), Lateral (or external) Pterygoid (LP), and Temporal (T). The rates between cross sectional areas of the muscles were used to write each one as a function of the force LP, resulting in the expressions in equation 1.

$$\begin{aligned} M &= 1,72LP \\ MP &= 1,15LP \\ T &= 0,99LP \end{aligned} \tag{1}$$

In previous works[6,7,8], a similar methodology was used by the group for developing the models. The boundary conditions here are such that relative displacements along the 1-2 line (Figure 3) are restricted, while in previous works the assumption that inwards displacement of the mandible at the region of the condyles was allowed. Another distinct feature is the consideration of horizontal loads, allowing the discussion of non-axial loading.

The two condyles were taken as supports, while an additional restraint on the frontal upper part of the mandible was used to avoid unbalanced forces resulting from approximations and numerical round ups. The constraints in points 1 and 2 of Figure 2 restrict local displacements in x, y and z, while point three fixes the displacements in z direction. By balancing the moments around axis 1-2, one obtains:

$$2M \times r_M + 2MP \times r_{MP} + 2T \times r_T + 2LP \times r_{LP} + 100 \times r_{100} = 0 \tag{2}$$

Substitution of (1) in (2), together with the consideration of the directional cosines in Table 2 and the relative distances r_i between muscle location and 1-2 axis given in Table 3 allows the calculation of force values for the horizontal and vertical external loadings (Table 4).

Forces	cos α		cos β		cos γ	
	Left	Right	Left	Right	Left	Right
Masseter	-0,043	0,043	-0,011	-0,011	0,999	0,999
Middle Pterygoid	0,587	-0,587	-0,165	-0,165	0,792	0,792
Lateral Pterygoid	0,714	-0,714	-0,692	-0,692	-0,106	-0,106
Temporalis	-0,325	0,325	0,219	0,219	0,920	0,920
100 (horizontal)	-0,907		0,420		0	
100 (vertical)	0		-1		0	

Table 2: Directional cosines for muscular forces.

Distance Vector	x (mm)	y (mm)	z (mm)
r_M	0	28,066	33,013
r_T	0	30,612	5,270
r_{LP}	0	9,558	6,311
r_{MP}	0	27,672	38,967
r_{100}	0	65,187	28,171

Table 3: Distance vector projections.

Muscle Force (N)	Vertical Load	Horizontal Load
M	49,251	8,907
PM	32,929	5,955
PL	28,634	5,178
T	28,348	5,127

Table 4: Force resultants for horizontal and vertical forces.

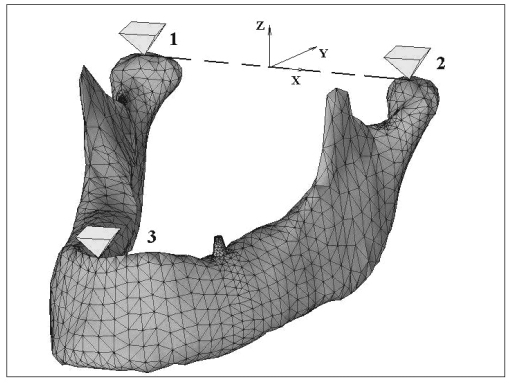

Figure 2: Boundary conditions.

The point of application of the loads followed the location of each muscle, as shown in Figure 3. Masseter and middle pterygoid action was evenly distributed in the contact area as shown in Figure 4, while for the other muscular forces, as they act in a much reduced surface and are distant from the region of interest for the analysis, were considered to be nodal.

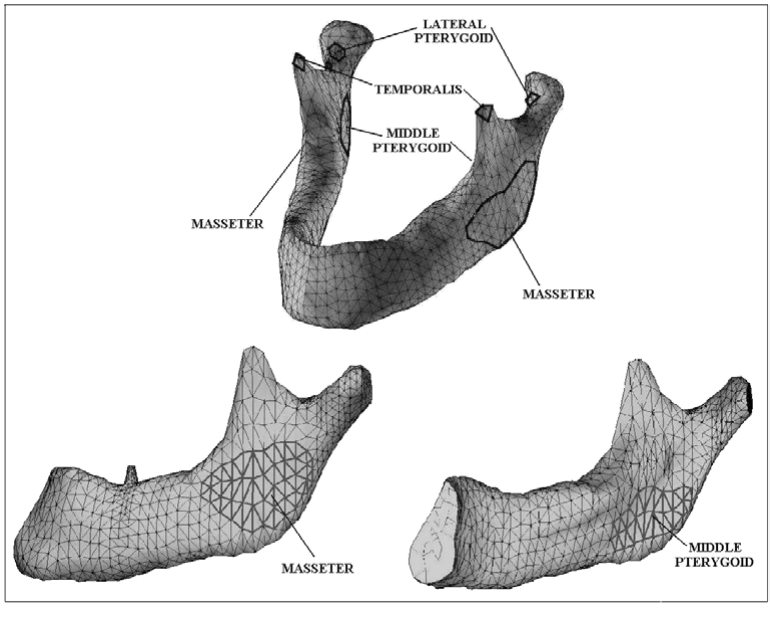

Figure 3: Points of load application.

4 RESULTS

The finite element solution for the model resulted in the principal stresses shown in Figures 5 to 12, showing the stress distribution in the implant-bone interface along a mesial-distal and a buccal-lingual section. The interfaces are shown in Figure 4: line 1-2-3 for the buccal-lingual boundary and 4-2-5 for the mesial-distal interface.

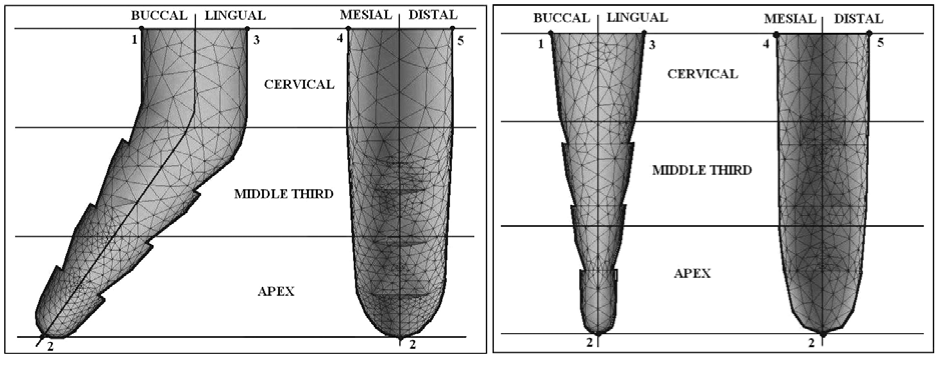

Figure 4: Contour lines for stress analysis of angled (a) and vertical implants.

Tables 5 and 6 summarize the obtained results, including maximum and minimum values for the stresses, as well as their location.

Vertical Load					
Section	Implants	σ_1		σ_3	
		MPa	Region	MPa	Region
buccal/lingual	Angled	2,74	cervical/lingual	-12,50	cervical/buccal
	Vertical	2,80	cervical/buccal	-8,10	cervical/lingual
mesial/distal	Angled	2,00	cervical/distal	-11,90	cervical/distal
	Vertical	1,30	cervical/distal	-10,00	cervical/mesial

Table 5 – Maximum stresses under vertical loading.

Horizontal Load					
Section	Implants	σ_1		σ_3	
		MPa	Region	MPa	Region
buccal/lingual	Angled	80,00	cervical/buccal	-76,00	cervical/lingual
	Vertical	70,00	cervical/buccal	-72,00	cervical/lingual
mesial/distal	Angled	12,50	cervical/distal	-12,00	cervical/distal
	Vertical	14,60	cervical/distal	-13,10	Cervical/distal

Table 6 – Maximum stresses under horizontal loading.

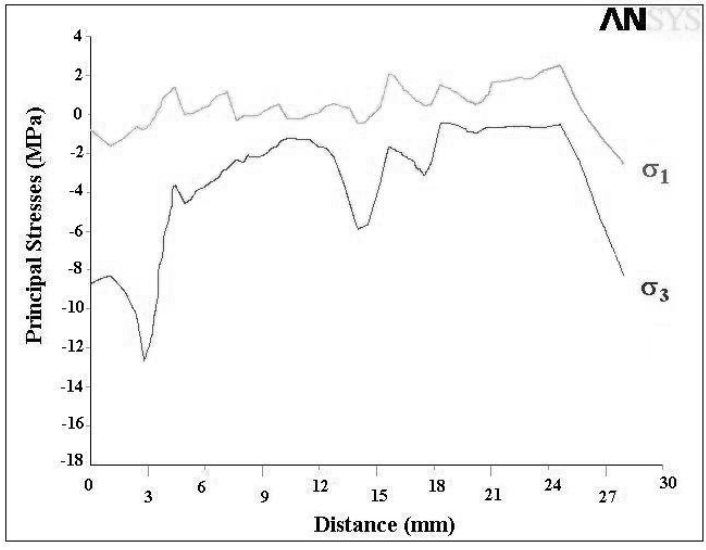

Figure 5: Principal stresses σ_1 and σ_3 in buccal-lingual section, angled implant under vertical load.

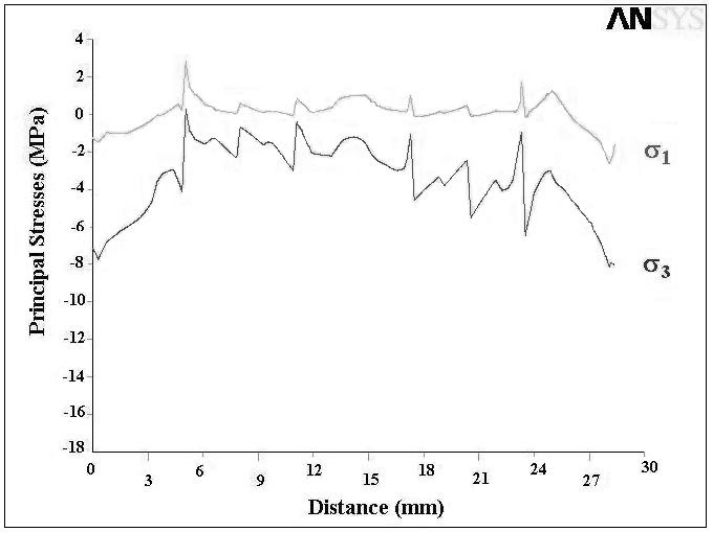

Figure 6: Principal stresses σ_1 and σ_3 in buccal-lingual section, vertical implant under vertical load.

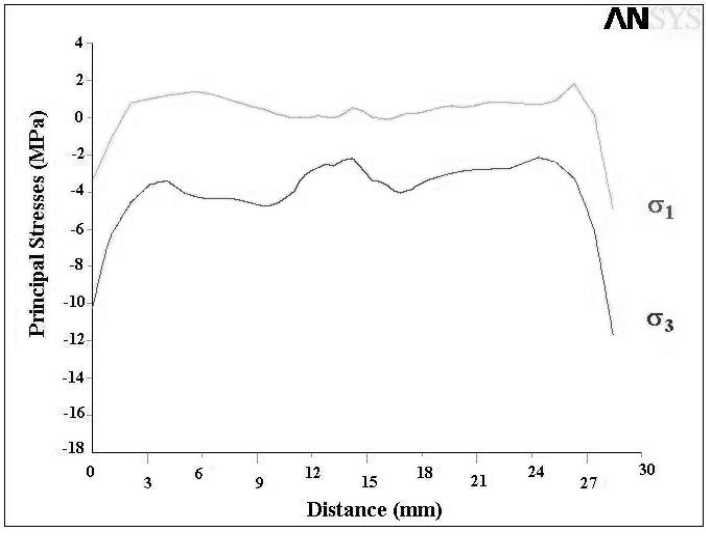

Figure 7: Principal stresses σ_1 and σ_3 in mesial-distal section, angled implant under vertical load.

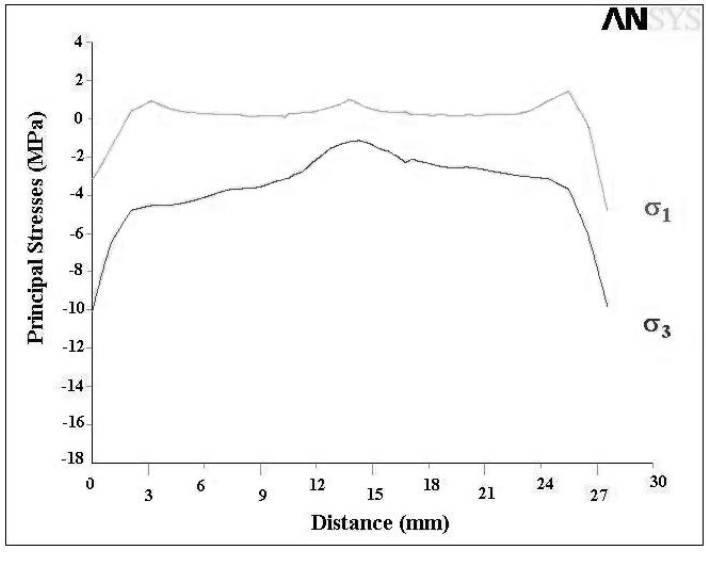

Figure 8: Principal stresses σ_1 and σ_3 in mesial-distal section, vertical implant under vertical load.

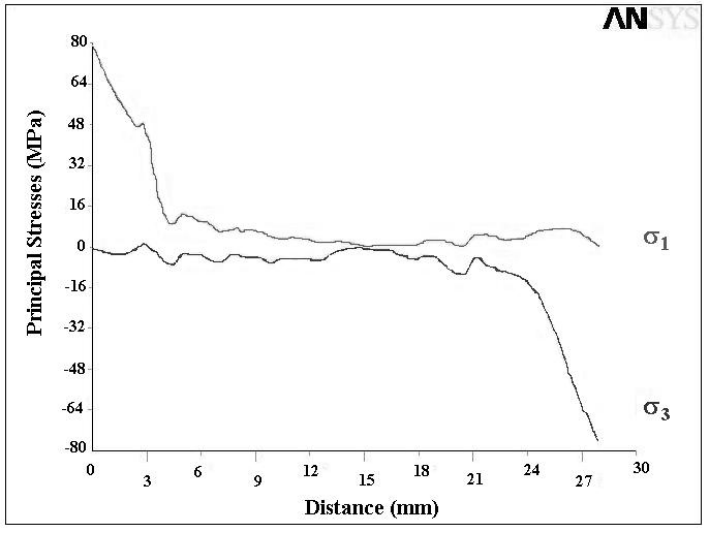

Figure 9: Principal stresses σ_1 and σ_3 in buccal-lingual section, angled implant under horizontal load.

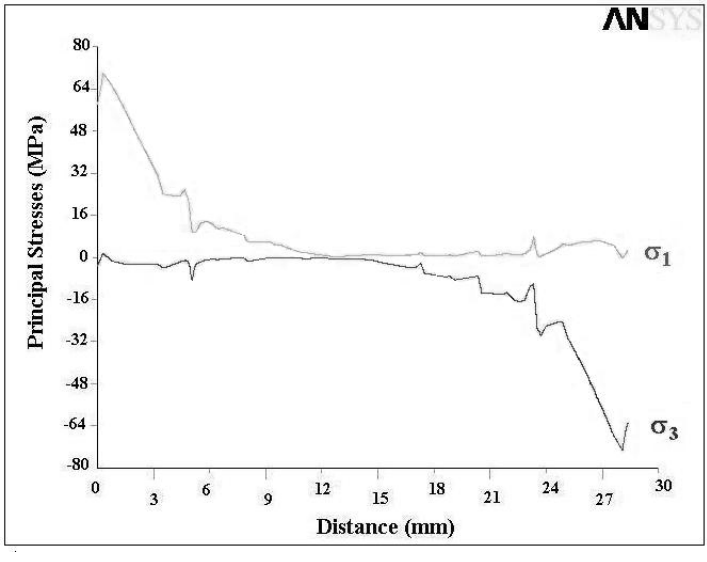

Figure 10: Principal stresses σ_1 and σ_3 in buccal-lingual section, vertical implant under horizontal load.

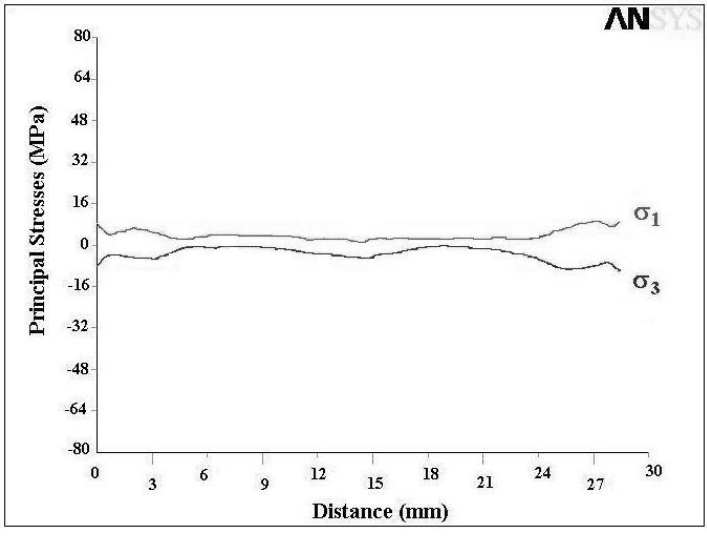

Figure 11: Principal stresses σ_1 and σ_3 in mesial-distal section, angled implant under horizontal load.

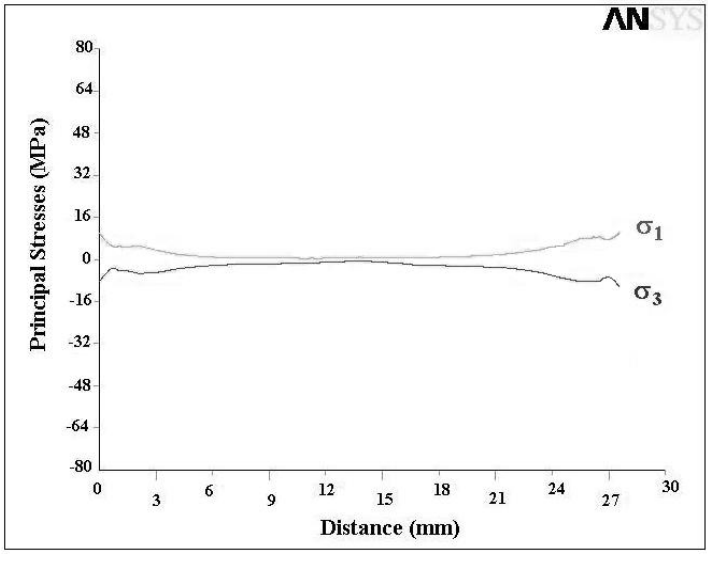

Figure 12: Principal stresses σ_1 and σ_3 in mesial-distal section, vertical implant under horizontal load.

For the angled implant under vertical loading, the tensile stresses occurred at the larger curvature region (lingual side, cervical region) and the compressive region corresponds to the portion with smaller curvature (buccal side, cervical region). For the vertical implant under vertical load, compressive stresses dominate, reaching its peak at the cervical region.

As for horizontal loading, the mechanical behavior of both implants is quite similar. The resulting bending, as expected, produces compressive stresses in the buccal region and tension at the lingual portion.

The mesial-distal cross section did not show significant changes for the two implant types, except for σ_3. The maximum compressive stress distribution shows a slight increase in the bent portion of the angled implant.

The most relevant difference was detected for vertical loading. Figure 13, which shows the level of principal stresses in the buccal-lingual cross section that cuts the implant axis, shows the regions were this difference is more pronounced, reaching around 50% increase for σ_3 at the concave (buccal) portion of the angled implant.

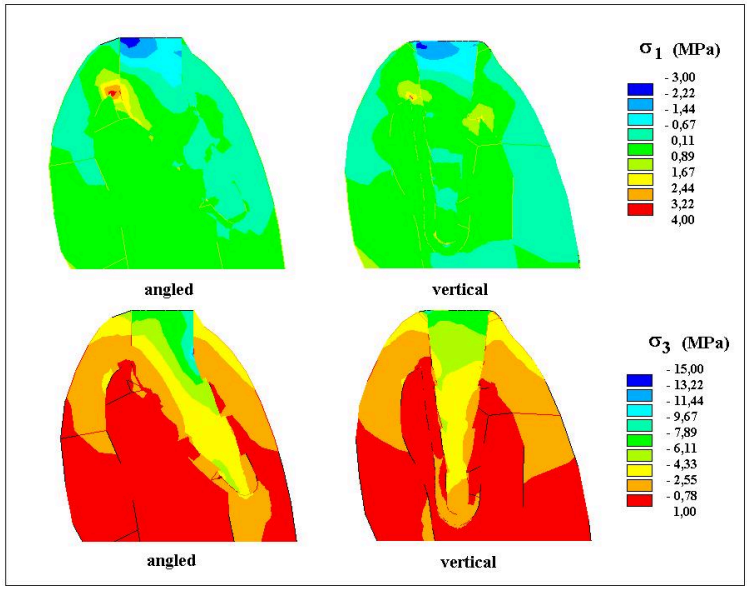

Figure 13: Principal stress distribution in buccal-lingual cross section.

5 CONCLUSION

Comparison with clinical or numerical analysis was not possible due to the innovative concept of the angled implant. Canay and co-workers[9] reported two-dimensional analysis of vertical and angled implants of the ITI Bonefit system; nevertheless, the angled implants have

their inclined part outside the bone, differently from the present case, being recommended for quite different problems and submitted to different stresses.

Stresses in the angled implant were higher than in vertical model. This fact was expected, as the indication of use of such model comes from occasional difficulties in the use of more traditional solutions. The larger differences in stresses were for vertical loading, reaching 25% for peak compressive stresses. Much higher stress values as expected occurred under horizontal loading, for both designs. It should be noted that in normal function, during mastication, the vertical components of the loading are significantly higher than the horizontal components. As for parafunction, horizontal loads can be dominant, representing a critical situation.

The obtained results are not conclusive in terms of the clinical performance of the angled implant. Clinical data based on patient observation would be required to assess the comparative advantages of the proposed design in specific clinical pathologies. On the other side, it should be noted that stresses resulting from occlusion and mastication are determining factors in the study of the success of osseointegration in dental implantology.

6 REFERENCES

[1] T. Albrektsson, G. Zarb, P. Worthington and A. R. Eriksson, "The long-term efficacy of currently used dental implants: a review and proposed criteria of success", *Int. J. Oral Maxillofac. Implants,* **1**, 11-25, (1986).

[2] G. F. Sodré, "Análise de Tensões em Implantes Odontológicos via Método dos Elementos Finitos", M. Sc. thesis, Universidade Federal de Minas Gerais, Belo Horizonte, (1999).

[3] H. Iplikçioglu, K. Akça, "Comparative evaluation of supporting three-unit fixed partial protheses on stress distribution in the bone", *Journal of Dentistry*, **30**, 41-46, (2002).

[4] P. P. van Zyl, N. L. Grundling, C. H. Jooste and E.Terblance, "Three-Dimensional Finite Element Model of a Human Mandible Incorporating Six Osseointegrated Implants for Stress Analysis of Mandibular Cantilever Protheses", *International Journal Oral and Maxillofacial Implants*, **10**, 51-57, (1995).

[5] N. Inou, H. Y. Fujiwara and K. Maki, "Functional Adaptation of Mandibular Bone", *Computational Biomechanics*, Springer-Verlag, 23-42, (1996).

[6] L. P. S. Barra, E. M. Toledo, M. Cruz and A. C. C. Lemonge, "Análise de Tensões na Vizinhança de um implante Bioform", COBEM, CD-ROM, (2001).

[7] M C. A. Cruz, "Análise tridimensional de tensões em torno do implante cuneiforme pelo Método dos Elementos Finitos", M. Sc. thesis, Universidade Camilo Castelo Branco, Campinas, (2001).

[8] P. C. Ferreira, R. B. Mendes, L. P. S. Barra and E. M. Toledo, "Análise de tensões em implantes odontológicos", *Principia – Caminhos da Iniciação Científica,* Editora da UFJF, **6**, 13-22, (2002).

[9] S. Canay, N. Hersek, I. Akpinar and Z. Asik, "Comparison of stress distribution around vertical and angled implants with finite element analysis", *Quintessence International*, **27**, 591-598, (1996).